

See discussions, stats, and author profiles for this publication at:
<https://www.researchgate.net/publication/260453457>

Collisional deactivation of $N_2(C\ 3\Pi_u, v=0, 1, 2, 3)$ states by N_2 , O_2 , H_2 and H_2O molecules

ARTICLE in CHEMICAL PHYSICS · DECEMBER 2000

Impact Factor: 1.65 · DOI: 10.1016/S0301-0104(00)00338-4

CITATIONS

85

READS

77

3 AUTHORS, INCLUDING:



Sergey Pancheshnyi

ABB

71 PUBLICATIONS 1,148 CITATIONS

SEE PROFILE

Collisional deactivation of $N_2(C^3\Pi_u, v = 0, 1, 2, 3)$ states by N_2 , O_2 , H_2 and H_2O molecules

S.V. Pancheshnyi^{*}, S.M. Starikovskaia, A.Yu. Starikovskii

Moscow Institute of Physics and Technology, Institutskii lane 9, Dolgoprudny, Moscow region, 141700 Russian Federation

Received 26 January 2000; in final form 4 October 2000

Abstract

The radiative lifetimes of four low vibration levels of the $N_2(C^3\Pi_u)$ state are measured and rate constants of collisional deactivation of these states by N_2 , O_2 , H_2 and H_2O molecules are determined with the help of emission spectroscopy. To excite levels under study a high-voltage nanosecond periodic discharge is used. © 2000 Published by Elsevier Science B.V.

Keywords: Quenching; Deactivation; Kinetics; Nitrogen; Second positive system; Vibrational levels; Nanosecond discharge; Fast ionization wave

1. Introduction

One of the serious problems of plasma chemistry is the high uncertainty in rate constants of elementary processes and chemical reactions under conditions of gas discharge. First of all, it is caused by the fact that there are not enough data relating to cross-sections of gas excitation by electron impact in discharge. The approach to description of gas excitation in various plasma-chemical systems can be developed via the analysis of the population dynamics of reference levels for which rate constants of population by electron impact and following depopulation are well known. One such reference level is the $C^3\Pi_u$ state of N_2 ; its population determines radiation intensity of the 2^+ nitrogen system (transition $C^3\Pi_u \rightarrow B^3\Pi_g$) in

discharges with N_2 . The short radiative lifetime ($\tau \sim 40$ ns) and relatively high excitation rate of this level make this transition suitable for diagnostics of the stationary plasma as well as the development of impulsive discharges. Analysis of population rate of the $N_2(C^3\Pi_u)$ state along with measurements of absolute radiation intensity of the 1^- system $N_2^+(B^2\Sigma_u^+ \rightarrow X^2\Sigma_g^+)$ makes it possible to reconstruct mean electron energy and concentration in the discharge. Deactivation rates of upper levels of associated transitions in various mixtures are, however, required to be well known to increase the accuracy of interpretation of experimental data.

In this study, the lifetimes and rate constants of deactivation of $N_2(C^3\Pi_u, v = 0, 1, 2, 3)$ vibration levels by molecules N_2 , O_2 , H_2 and H_2O in the ground state are determined with the help of emission spectroscopy with subnanosecond temporal resolution. Impulsive discharge at low pressure in the form of fast ionization wave (FIW) was

^{*} Corresponding author. Tel./fax: +7-095-408-6347.

E-mail address: pon@neq.mipt.ru (S.V. Pancheshnyi).

used to excite levels under study. Earlier [1], this method was used to determine the radiative lifetime and rate constants of deactivation of states $N_2(C^3\Pi_u, v=0)$ and $N_2^+(B^2\Sigma_u^+, v=0)$ by N_2 , O_2 , H_2 , CO and H_2O molecules.

2. Experimental setup

Fig. 1 shows the scheme of experimental setup and diagnostics system. FIW was initiated by negative polarity voltage impulses of 15 kV amplitude, 25 ns duration at half-maximum, 3 ns rise time and 40 Hz repetition frequency. The pulses were transported from the high-voltage generator to the high-voltage electrode of the discharge tube through a 50 Ω coaxial cable. The discharge device comprised a glass tube of 17.5 mm inner diameter, 21.5 mm outer diameter and 600 mm length at which ends electrodes of stainless steel were located. The tube was surrounded by a metal screen of 60 mm diameter. It was able to pump down the vacuum system to a pressure of $\sim 10^{-4}$ Torr with the help of forevacuum and diffusion pumps. Pressure of the gas studied was measured by a U-tube oil pressure gauge. Emission was recorded by the optical system that consists of a set of diaphragms, monochromator MDR-12A and photomultiplier 14ELU-F7S. The emission was selected in the direction perpendicular to the discharge device axis at the distance of 20 ± 2 cm from

the high-voltage electrode. Signals were recorded using oscilloscope Tektronix TDS-380. Spectral range of the optical system was $\lambda = 250$ –600 nm, temporal resolution was better than $\tau \simeq 1$ ns.

3. Measurements

Measurements were performed in spectrally pure nitrogen (99.999%, main impurities: CH_4 , CO_2 , CO) and its mixtures with investigated molecules – $N_2:O_2$ (4:1), $N_2:H_2$ (9:1) and $N_2:H_2:O_2$ (4:2:1) at pressures ranging from 0.05 to 30 Torr and at a temperature of 295 ± 5 K.

To record the temporal dynamics of molecular nitrogen states under study the vibrational transitions of the second positive system $N_2(C^3\Pi_u, v') \rightarrow N_2(B^3\Pi_g, v'')$ were chosen. Fig. 2a shows the emission spectrum of the discharge in pure nitrogen at $P = 4$ Torr. The main criterion to choose one or another transition was the possibility to reliably separate the associated molecular emission band. As a result of performed analysis, measurements were performed at wavelengths corresponding to $0 \rightarrow 0$ (337.1 nm), $1 \rightarrow 0$ (315.9 nm), $2 \rightarrow 1$ (313.6 nm), $3 \rightarrow 7$ (414.2 nm) transitions of the second positive system of nitrogen. To exclude the influence of rotational relaxation, emission from the whole rotational–vibrational band was registered. At that, bandwidth for each transition was determined experimentally.

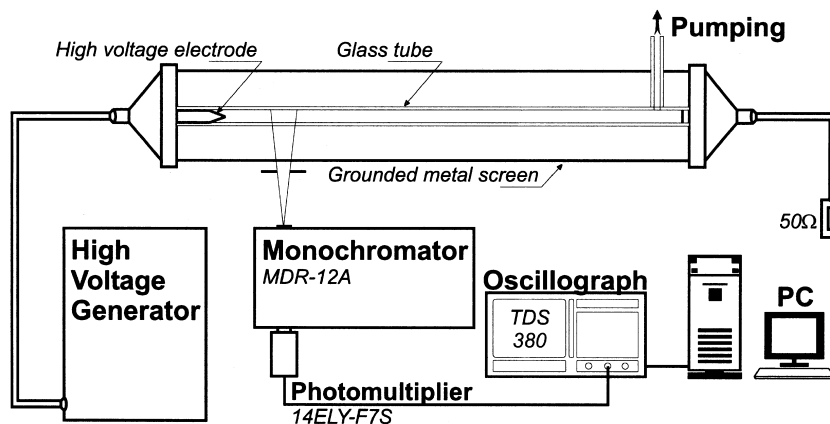


Fig. 1. Experimental setup.

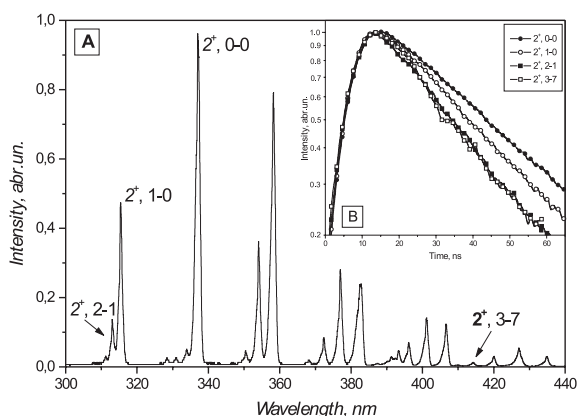


Fig. 2. (a) Radiation spectrum of discharge in pure nitrogen at $P = 4$ Torr. (b) Characteristic semi-logarithmic oscillograms of emission at the same conditions.

Temporal dependence of the emission $I(t)$ of the transitions under study in pure nitrogen at $P = 4$ Torr pressure is given in Fig. 2b. As it follows from the figure, a region of monoexponential decrease of the emission follows after a zone of intensive excitation (taking place up to $t_0 = 25$ ns at 1 Torr pressure and up to $t_0 = 5$ –6 ns at high pressures):

$$I(t) = I_0 \exp\left(-\frac{t}{\tau}\right) \quad \text{at } t > t_0 \quad (1)$$

FIW refers to propagation of high ionization region through the discharge gap. High propagation velocity $V \sim 10^9$ cm s $^{-1}$, spatial uniformity and good repeatability are caused by high electric field in the wave front $(E/N)_{\max} \sim 10^3$ Td, half-field peak width $t_{1/2} \simeq 2$ –5 ns, which provide high uniformity of gas preionization and ionization in the wave front and ahead of it [2]. As demonstrated in Ref. [3], most of the ionization and excitation of the gas takes place in residual electric fields ($E/N \sim 10^2$ Td) behind the FIW front. It should be emphasized that due to the short time of gas excitation (up to 25 ns) both the degree of gas dissociation and the relative concentration of excited particles in a single impulse are in the order of $\alpha \sim 10^{-4}$, which makes it possible to disregard quenching of levels investigated in collisions with excited particles [4,5].

Conditions are somewhat different for the mixture $N_2:H_2:O_2$. A mixture of nitrogen with water vapor (at pressures no over the saturation pressure) is the state of thermodynamic equilibrium of the $N_2:H_2:O_2$ mixture at ambient temperature. The investigations performed have demonstrated that the complete hydrogen conversion under FIW conditions, which is observed by emission continuum $H_2(a^3\Sigma_g^+ \rightarrow b^3\Sigma_u^+)$ in high spectral band (250–400 nm) takes place under our conditions in the time period of about 3–5 min. This makes it possible to consider the discharge gas composition be close to the equilibrium one. In doing so, the H_2O vapor pressure was recalculated with the use of stoichiometric relations; if $[H_2]_{\text{ini}}$, $[O_2]_{\text{ini}}$ and $[H_2O]_{\text{fin}}$ are the initial concentrations of H_2 and O_2 molecules, and final density of H_2O respectively, then

$$[H_2O]_{\text{fin}} = [H_2]_{\text{ini}} = 2[O_2]_{\text{ini}}$$

Thus, the oxygen–hydrogen conversion into water molecules leads to the decrease in total pressure, and this fact was registered experimentally. More detailed analysis of hydrogen oxidation in the nanosecond discharge is represented in Ref. [6].

4. Discussion

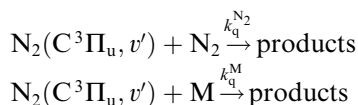
4.1. Collisional quenching by heavy particles

Specific times of gas relaxation lie in the range 10^{-3} – 10^{-5} s, as resulted from the analysis of the kinetic scheme with the process rate constants taken from Ref. [7]. Therefore, the accumulation of excited particles from one impulse to another is negligible. In this case, the dynamics of the levels population is determined by:

- population by direct electron impact from the ground state of nitrogen $N_2(X^1\Sigma_g^+, v=0)$

$$N_2(X^1\Sigma_g^+, v=0) + e \rightarrow N_2(C^3\Pi_u, v') + e$$
- emission of photons

$$N_2(C^3\Pi_u, v') \xrightarrow{1/\tau_0} N_2(B^3\Pi_g) + h\nu$$
- collisional deactivation



Herein τ_0 – radiative lifetime of the associated level, $k_q^{\text{N}_2}$ – rate constant of the excited molecule deactivation by N_2 molecules, k_q^{M} – rate constant of deactivation by M molecule, where $\text{M} = \text{O}_2$, H_2 or H_2O .

The droop of emission takes place in relatively moderate electric fields where processes of investigated level population by electron impact can be disregarded [3]. Thereby, the kinetic equation for excited particles $[\text{N}^*]$ can be written in the following form:

$$\frac{d[\text{N}^*]}{dt} = -\frac{1}{\tau_0}[\text{N}^*] - k_q^{\text{N}_2}[\text{N}_2][\text{N}^*] - k_q^{\text{M}}[\text{M}][\text{N}^*], \quad (2)$$

with the solution:

$$[\text{N}^*](t) = [\text{N}^*]_0 \exp\left(-\frac{t}{\tau}\right) \quad (3)$$

Herein $[\text{N}_2]$ and $[\text{M}]$ – concentration of associated molecules-deactivators, τ – lifetime observed in the experiment which is determined by all the processes:

$$\frac{1}{\tau} = \frac{1}{\tau_0} + k_q^{\text{N}_2}[\text{N}_2] + k_q^{\text{M}}[\text{M}] \quad (4)$$

If there is no reabsorption, the emission intensity $I(t)$ of the associated band is proportional to the upper level population $[\text{N}^*](t)$, which makes it possible to determine the gas pressure dependence of $1/\tau$ for the investigated levels in various mixtures in accordance with Eq. (3) (see Figs. 3 and 4). The values of the radiative lifetime τ_0 were obtained by extrapolation to zero pressure and the quenching rates k_q were determined from slope of the straight line $1/\tau$ vs. pressure (4).

Radiative lifetimes and deactivation rate constants obtained are shown in Tables 1 and 2, respectively. Comparison with results of previous selected studies is given therein.

The quality of the recorded signal introduces the greatest error in the results obtained. Application of statistical analysis makes it possible to decrease the error of the values obtained, on the

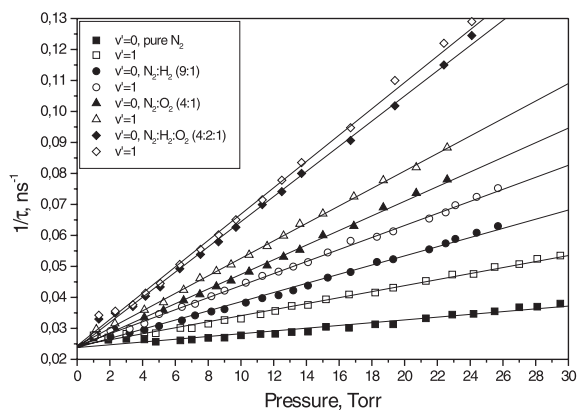


Fig. 3. Pressure dependence of observed lifetime of the levels $\text{N}_2(\text{C}^3\Pi_u, v=0)$ and $\text{N}_2(\text{C}^3\Pi_u, v=1)$ in various mixtures.

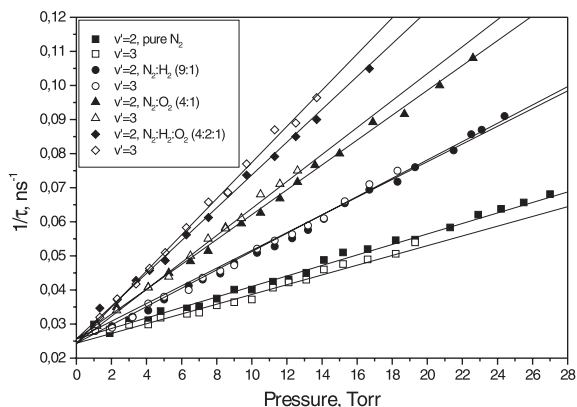


Fig. 4. Pressure dependence of observed lifetime of the levels $\text{N}_2(\text{C}^3\Pi_u, v=2)$ and $\text{N}_2(\text{C}^3\Pi_u, v=3)$ in various mixtures.

average, to 5–15%. It should be noted that heating of the working mixture at average power consumption of 4.5 W was not over 5–10 K at an average temperature of 295 K.

Due to the fact that, as a rule, authors determine the radiative lifetimes and deactivation rate constants only for the first states of $\text{N}_2(\text{C}^3\Pi_u, v=0, 1)$, only some of them are given in the tables. Attention should be drawn to Refs. [8,9]. Using a pulsed proton beam at various pressures, the authors measured the radiative lifetimes of the excited states of nitrogen molecules. In this case the error of the result obtained is sufficiently low – less than 5%. The good coincidence

Table 1
Radiative lifetimes (in 10^{-9} s)

$N_2(C^3\Pi_u, v=0)$	$N_2(C^3\Pi_u, v=1)$	$N_2(C^3\Pi_u, v=2)$	$N_2(C^3\Pi_u, v=3)$	Reference
42 ± 2	41 ± 3	39 ± 4	41 ± 5	PW*
42 ± 2	41 ± 2	40 ± 2	36 ± 2	[8]
40.4 ± 0.5	40.6 ± 0.5	38.5 ± 0.6	–	[9]
30 ± 2	37 ± 3	–	–	[14]

PW* – Present work.

Table 2
Deactivation rate constants (in 10^{-10} cm³ s⁻¹)

Molecule	$N_2(C^3\Pi_u, v=0)$	$N_2(C^3\Pi_u, v=1)$	$N_2(C^3\Pi_u, v=2)$	$N_2(C^3\Pi_u, v=3)$	Reference
N_2	0.13 ± 0.02	0.29 ± 0.03	0.46 ± 0.06	0.43 ± 0.06	PW*
	0.109 ± 0.01	0.253 ± 0.03	0.413 ± 0.04	0.428 ± 0.04	[8]
	–	0.33 ± 0.04	0.63 ± 0.08	0.80 ± 0.20	[10]
	0.11 ± 0.06	0.27 ± 0.02	–	–	[14]
	0.113	0.259	–	–	[15]
O_2	3.0 ± 0.3	3.1 ± 0.3	3.7 ± 0.5	4.3 ± 0.6	PW*
	2.8 ± 0.2	3.0 ± 0.2	–	–	[14]
	2.7	3.0	–	–	[15]
H_2O	3.9 ± 0.4	3.7 ± 0.4	4.0 ± 0.6	4.5 ± 0.7	PW*
	4.1	4.0	–	–	[15]
H_2	3.3 ± 0.3	3.2 ± 0.3	3.7 ± 0.5	4.3 ± 0.6	PW*

PW* – Present work.

of the corresponding radiative lifetimes of levels investigated is one of criteria for the reliability of the results of this study.

Redetermination of quenching rate constants from the balance of population and deactivation of the level under consideration seems to be less reliable. For example, in the case of excitation by a silent discharge at pressures up to 1 atm [10] it is necessary to consider both vibrational distribution of nitrogen molecules in the ground state and electron energy distribution function (EEDF). Uncertainty in these distributions and, consequently in the population rates, can introduce a large error in measured rate constants. A high degree of dissociation and excitation also complicate the interpretation of experimental data.

Important advantages in the present work of using a nanosecond discharge as an excitation source, are the pulsed pumping of short duration at low repetition frequency, the moderate pressures and high spatial homogeneity.

4.2. Effect of excitation and deactivation of states under investigation by electron impact

Analysis of the FIW structure [3] showed that most of the gas excitation takes place behind the wave front in a region of relatively low electric fields. However, it was shown in Ref. [3] that relaxation of the EEDF in the energy range associated with inelastic processes ($\varepsilon > 10$ eV) proceeds for a time comparable with the time of radiative depopulation of investigated levels. Under conditions of the nanosecond discharge, electrons with high energy formed in the wave front region ($E/N \sim 10^3$ Td), do not thermalize during the time of radiative depopulation of corresponding levels at characteristic pressures of several Torr.

In this case, the additional population and depopulation of states investigated is possible, among others, in the superelastic processes with the participation of electrons. To analyze possible effect of $N_2(C^3\Pi_u)$ states excitation for a long

period of time, two sets of experiments with high-voltage excitation impulses of various duration were conducted: $\tau_1 = 25$ ns and $\tau_2 = 5$ ns.

Electric field structure, as well as density and mean energy of the electrons in the region of measurements, is essentially diverges in the first and second cases. Despite this fact, the measured radiative lifetimes coincide with each other within the experimental accuracy in the wide range of discharge development conditions at pressures from 4 to 30 Torr. This allows to make a conclusion about minor contributions of processes with participation of electrons in this range of parameters during the most active decay of the $N_2(C^3\Pi_u, v')$ vibrational states under conditions of our experiment.

Electron concentration and mean energy behind the electric field front vary relatively little with the decrease of pressure [2,3], which results in an increase of the relative contribution of processes with participation of excited particles and free electrons in the deactivation process. This effect most clearly exhibits itself in a change of the $\tau(P)$ dependence (Fig. 5). The linear relation between $1/\tau$ and P , which characterizes at $P > 4$ Torr the binary nature of deactivating collisions with specified efficiency (collision partner – N_2), is replaced at lower pressures with a complicated dependence, which gives an indication of the effective

deactivation rate constant increase in this range. The most likely reason for this acceleration of depopulation is an increase of electron concentration and the contribution of superelastic collisions in the process of collisional deactivation of the $N_2(C^3\Pi_u)$ state. The rate of such additional deactivation is directly proportional to the electron concentration n_e and rate constant k_-^{el} of the corresponding process:

$$\left(\frac{d[N^*]}{dt}\right)_{\text{elec}} = -k_-^{el}n_e[N^*]$$

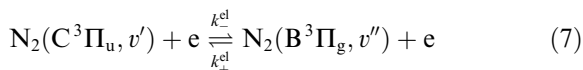
The equation that describes the observed lifetime of level v' is similar to Eq. (4) and can be written in the following form:

$$\frac{1}{\tau} = \frac{1}{\tau_0} + k_q^{N_2}[N_2] + k_q^M[M] + k_-^{el}n_e \quad (5)$$

The estimation of electron concentration in the discharge afterglow can be obtained using method described in Refs. [2,3] which provides $n_e \simeq 5 \times 10^{12} \text{ cm}^{-3}$ for $P = 2$ Torr. Suggesting that deactivation in collision with heavier particles takes place with similar efficiency in the whole range of pressures under investigation (in particular, this means that deactivation on excited components is disregarded), in accordance with data of Fig. 5 one can obtain for k_-^{el} :

$$k_-^{el}|_{\text{exp}} \simeq 4 \times 10^{-7} \text{ cm}^3 \text{ s}^{-1} \quad (6)$$

To separate the main channel of the additional deactivation it is interesting to compare the values found with the theoretical estimation. For transitions with participation of the $N_2(C^3\Pi_u, v')$ level, the second positive system transition of nitrogen is optically allowed and the following process will be the process with the maximum rate:



To determine rate constants, k_-^{el} and k_+^{el} , let us find the cross-section of the direct σ_- and reverse σ_+ processes (7). For this purpose Drawin's semi-empirical model [11] on the basis of Bethe-Born approximation with corrections [12] and the principle of detailed balance are used:

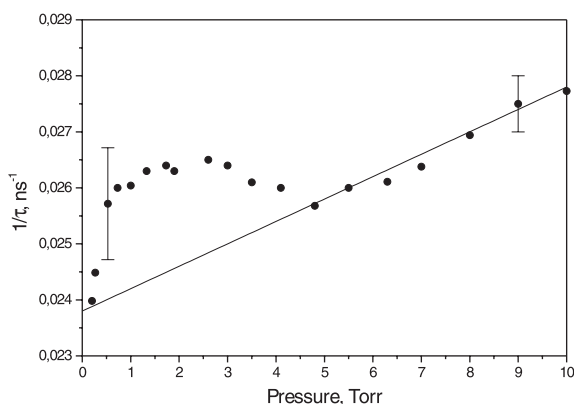


Fig. 5. Dependence of observed lifetime of the level $N_2(C^3\Pi_u, v = 0)$ in pure nitrogen at low pressures.

$$\sigma_+(\varepsilon) = 4\pi a_0^2 f \left(\frac{\text{Ry}}{w} \right)^2 \times \left(\frac{u}{(u+1)^2} \ln[1.25(u+1) + 1] + \frac{X}{u+1} \right)$$

$$\sigma_-(\varepsilon) = \sigma_+(\varepsilon + w) \frac{g^-}{g^+} \frac{\varepsilon + w}{\varepsilon}$$

Here, a_0 – Bohr’s radius, Ry – Rydberg’s constant, w – energy and $f = 0.046$ – oscillator strength of transition, $u = (\varepsilon - w)/w$ – dimensionless variable, $X = 0.1$ – model parameter, g^-/g^+ – ratio of statistical weights of lower and upper states, respectively.

Such approach disregards the vibrational structure of electronic levels and can only be used for the estimation of quenching rate by an order of magnitude. It should be noted that more accurate calculations on the basis of Frank–Condon principle lead to insignificant (not more than by a factor of 3) difference, but necessitate vibrational distribution of excited molecules of nitrogen.

To calculate rate constant of a process, using known cross-section, it is necessary to know the EEDF. It was shown in Ref. [3] that in the FIW front the electron distribution is highly non-equilibrium. However, to obtain an estimation even in the early afterglow, the low-energy part of EEDF can be approximated by Maxwell’s distribution with good accuracy. At conditions used in this paper the electron concentrations behind the FIW front is $n_e \simeq 5 \times 10^{12} \text{ cm}^{-3}$, mean electron energy – $T_e \simeq 1 \text{ eV}$. Both values vary relatively weakly with a pressure. The associated rate constants of the direct k_-^{el} and reverse k_+^{el} processes for Eq. (7) are equal:

$$k_-^{\text{el}}|_{\text{theor}} \sim 10^{-7} \text{ cm}^3 \text{ s}^{-1}$$

$$k_+^{\text{el}}|_{\text{theor}} \sim 10^{-9} \text{ cm}^3 \text{ s}^{-1} \quad (8)$$

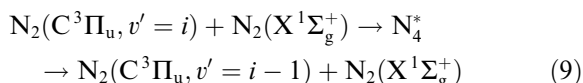
At the conditions of nanosecond gas discharge at low pressure the total population of $\text{N}_2(\text{C}^3\Pi_u)$ state exceeds one for the $\text{N}_2(\text{B}^3\Pi_g)$. Thereby, in the afterglow, where the average electron energy decreases to 1 eV, the rate of the $\text{N}_2(\text{C}^3\Pi_u)$ excitation becomes negligibly low in comparison with the rate of deactivation of this state by electrons.

Estimation obtained (8) is in a good agreement with the measured value (6). Thus, quenching by electrons is the additional deactivation process at the FIW conditions. On the other hand, this effect can only be observed at relatively high electron concentration in plasma, at low pressures, when the degree of gas ionization α_{ion} exceeds the ratio of rate constants of the quenching by heavy particles and electrons.

At the conditions of our study, the critical ratio about $\alpha_{\text{ion}}^* \sim 10^{-3}$ is only achieved at pressures below 4 Torr. At high pressures the degree of gas ionization linearly decreases that allows to neglect of quenching by electrons.

4.3. Analysis of vibration relaxation effect

Authors of Ref. [13] discuss the possibility of additional vibration relaxation of the $\text{N}_2(\text{C}^3\Pi_u, v')$ states in the process of the pure vibrational relaxation:



Denote the rate constant of process (9) for i state as $k_{i,i-1}^{\text{vibr}}$ and deactivation rate constant with a transition to another electron level as $k_i^{\text{N}_2}$. Effective constant k_i^{eff} observed in pure nitrogen can be written as:

$$k_i^{\text{eff}} = k_i^{\text{N}_2} + k_{i,i-1}^{\text{vibr}} \times \left(1 - \frac{k_{i+1,i}^{\text{vibr}} [\text{N}_2(\text{C}^3\Pi_u, v' = i + 1)]}{k_{i,i-1}^{\text{vibr}} [\text{N}_2(\text{C}^3\Pi_u, v' = i)]} \right)$$

for $i \neq 0$ (10)

$$k_i^{\text{eff}} = k_i^{\text{N}_2} - k_{i+1,i}^{\text{vibr}} \times \frac{[\text{N}_2(\text{C}^3\Pi_u, v' = i + 1)]}{[\text{N}_2(\text{C}^3\Pi_u, v' = i)]} \quad \text{for } i = 0 \quad (11)$$

In this case, insofar as the experimentally observed rate constants of vibration state depopulation remarkably increase with the level number i (Table 2), contribution of the VT-relaxation flow should result in non-monoexponential behavior of emission profile for transitions from lower vibration levels of $\text{N}_2(\text{C}^3\Pi_u, v')$.

The upper estimation of the VT-relaxation flow can be obtained from Eq. (11) and experimentally measured ratio of concentrations of the $N_2(C^3\Pi_u, v=0)$ and $N_2(C^3\Pi_u, v=1)$ levels using expression for emission intensity $I_{v'v''}$ of vibrational transition $v' \rightarrow v''$:

$$I_{v'v''} = \zeta(v) h \nu_{v'v''} \frac{[N^*]}{\tau_0} \frac{q_{v'v''}^3 \nu_{v'v''}^3}{\sum_{v''} q_{v'v''}^3 \nu_{v'v''}^3} \quad (12)$$

Herein $\zeta(v)$ – coefficient of the spectral sensitivity and geometrical factor of the experimental setup, $\nu_{v'v''}$ – transition frequency, $q_{v'v''}$ – Frank–Condon's coefficients.

Eq. (12) relates emission intensity of the transitions to the population of the associated levels. In this study, radiation profiles of all the vibration levels of the $N_2(C^3\Pi_u, v')$ state (Fig. 2) were analyzed.

In the pressure range under study the ratio of peak populations of the vibration levels relatively weakly depends on pressure. Characteristic value at $P = 4$ Torr made up $[v' = 0]:[v' = 1]:[v' = 2]:[v' = 3] = 1.00:0.73:0.25:0.12$. It was shown that in the afterglow concentration profiles of all the levels are monoexponential within the accuracy of experiment, which allows to impose an upper limitation to the rate constant of vibration relaxation:

$$k_{1,0}^{\text{vibr}} \leq 5 \times 10^{-12} \text{ cm}^3 \text{ s}^{-1} \quad (13)$$

Authors of Ref. [13] gave the following values:

$$\begin{aligned} k_{1,0}^{\text{vibr}} &= (1.6 \pm 0.5) \times 10^{-11} \text{ cm}^3 \text{ s}^{-1} \\ k_{2,1}^{\text{vibr}} &= (1.1 \pm 0.3) \times 10^{-11} \text{ cm}^3 \text{ s}^{-1} \end{aligned} \quad (14)$$

These data are in the notable disagreement with the estimation obtained in this study. In particular, data of Ref. [13] leads to conclusion that the rate of the $N_2(C^3\Pi_u, v')$ depopulation with a transition to another excited state and the rate of the $N_2(C^3\Pi_u, v')$ depopulation with a vibrational number change only are close values.

On the contrary, the estimation obtained in this study demonstrates that the process of vibrational relaxation within the $N_2(C^3\Pi_u)$ state is always negligible in comparison with the depopulation with a change of the electronic state.

The reason for such discrepancy is a set of assumptions made in Ref. [13]. In particular, in formulation of the data processing procedure it was suggested that the radiative lifetimes and rate constants of collisional deactivation with the electronic state change for all vibration levels are equal. On the other hand, values of k_q which differ for various levels in about three times are given; this asserts to that there is no self-consistency of analysis performed in Ref. [13]. It should be noted that to determine more accurately constants of the vibrational exchange $k_{i,i-1}^{\text{vibr}}$ it is necessary to use techniques of selective excitation of the $N_2(C^3\Pi_u, v')$ vibration levels.

5. Conclusion

In this study the radiative lifetimes of the $N_2(C^3\Pi_u, v=0, 1, 2, 3)$ states are measured and the rate constants of collisional deactivation of these states by N_2 , O_2 , H_2 and H_2O molecules are determined using the emission spectroscopy method. A range of parameters at which it is necessary to take into account superelastic collisions of excited particles with the free electrons is revealed. The analysis performed also demonstrates slight contribution of the vibrational relaxation in the rate of collisional deactivation of the $N_2(C^3\Pi_u, v')$ levels.

Acknowledgements

This study was partially supported by the Russian Foundation for Basic Research (project 99-03-32237), INTAS (96-2110) and US Air Force Research Laboratory's Office of Scientific Research, European Office of Aerospace Research and Development, London, UK (SPC-99-4007).

References

- [1] S.V. Pancheshnyi, S.M. Starikovskaia, A.Yu. Starikovskii, Chem. Phys. Lett. 294 (1998) 523.
- [2] N.B. Anikin, S.V. Pancheshnyi, S.M. Starikovskaia, A.Yu. Starikovskii, J. Phys. D: Appl. Phys. 31 (1998) 826.

- [3] S.V. Pancheshnyi, S.M. Starikovskaia, A.Yu. Starikovskii, *J. Phys. D: Appl. Phys.* 32 (1999) 2219.
- [4] S.M. Starikovskaia, *Plasma Phys. Rep.* 21 (1995) 541 (in Russian).
- [5] N.B. Anikin, S.M. Starikovskaia, A.Yu. Starikovskii, *Plasma Phys. Rep.* 26 (2000) 606.
- [6] D.V. Zatspin, S.M. Starikovskaia, A.Yu. Starikovskii, 14th International Symposium on Plasma Chemistry, vol. II, Prague, Czech Republic, 1999, 927.
- [7] V. Guerra, J. Loureiro, *Plasma Sources Sci. Technol.* 6 (1997) 373.
- [8] C.H. Chen, M.G. Payne, G.S. Hurts, J.P. Judish, *J. Chem. Phys.* 65 (1976) 3863.
- [9] L.W. Dotchen, E.L. Chupp, D.J. Pegg, *J. Chem. Phys.* 59 (1973) 3960.
- [10] E. Gat, N. Gherardi, S. Lemoing, F. Massines, A. Ricard, *Chem. Phys. Lett.* 306 (1999) 263.
- [11] H.W. Drawin, F. Emard, *Physica* 85 (1977) 333.
- [12] G.G. Chernyi, S.A. Losev (Eds.), *Physical–Chemical Processes in Gas Dynamics*, MSU Press, Moscow, 1995 (in Russian).
- [13] J.M. Calo, R.C. Axtmann, *J. Chem. Phys.* 54 (1971) 1332.
- [14] P. Millet, Y. Salamero, H. Brunet, J. Galy, D. Blanc, J.L. Teyssier, *J. Chem. Phys.* 58 (1973) 5839.
- [15] F. Albugues, A. Birot, D. Blanc, H. Brunet, J. Galy, P. Millet, J.L. Teyssier, *J. Chem. Phys.* 61 (1974) 2695.